Vol 13 No 9, September 2004
1009-1963/2004/13(09)/1564-05

Chinese Physics

© 2004 Chin. Phys. Soc.
and IOP Publishing Ltd

The dissociative ionization and Coulomb explosion of ethane by a femtosecond laser field*

Li Xia(李 霞), Ren Hai-Zhen(任海振), Ma Ri(马 日),
Chen Jian-Xin(陈建新), Yang Hong(杨 宏), and Gong Qi-Huang(龚旗煌)†

State Key Laboratory for Mesoscopic Physics, Department of Physics, Peking University, Beijing 100871, *China*

(Received 9 January 2004; revised manuscript received 10 May 2004)

Femtosecond laser-induced dissociation and Coulomb explosion of polyatomic molecule C_2H_6 were systematically investigated using a time-of-flight mass spectrometer and a chirped pulse amplifier laser. With the laser intensity varying from 2.4×10^{15} W/cm^2 to 1.2×10^{16}W/cm^2, strong molecular ions $C_2H_n^+$ (n=0–6) and atomic ions C^{m+} (m=1–3) signals were observed. The double-peak structure of atomic ions indicated the occurrence of Coulomb explosion. Compared with the nearly isotropic distribution of C^+, highly charged ions C^{m+} (m=2–3) exhibited a sharply anisotropic angular distribution, which was attributed to the geometric alignment.

Keywords: field ionization, multiphoton processes, mass spectra
PACC: 7970, 3280K, 3520X

1. Introduction

The interaction of intense lasers with atoms and molecules has been of continuing interest in recent years.[1−7] When the laser intensity reaches 10^{15}W/cm^2, the electric field of the laser is comparable to the Coulombic field felt by the valence electron. Several valence electrons may be stripped away if the molecules are subjected to such an intense laser field. The removal of more than one electron leads to the Coulomb explosion of the molecule into multicharged atomic ions. Over the past years, experiments have indicated that the kinetic energy of all fragment ions accounts for a substantial fraction (∼70% for Cl_2 and I_2, ∼45% for N_2, CO and O_2) of the Coulomb explosion energy for all final charge states, regardless of the pulse rise time.[7,8] In the diatomic case, the Coulomb explosion energy is given by the expression $E_e = Q_1Q_2/R_e$ (in atomic unit), where Q_1 and Q_2 are the atomic ion charges and R_e is the equilibrium internuclear separation of the neutral molecules. Posthumus *et al*[9−11] used the refined field-ionization Coulomb explosion model to reproduce the multielectron dissociative ionization (MEDI) data of iodine remarkably well. Other models such as the two-step model[12] and the Thomas–Fermi–Dirac (TFD) model[13] have been proposed to explain the kinetic energy release (KER) in the Coulomb explosion process. The main point in all these models is that the molecule (molecular ion) relaxes to R_c, the so-called critical internuclear distance, where it is stabilized and subsequently ionized, with little or no change in interion separation for the different ionization stages.

The angular distributions of fragment ions ejected from the Coulomb explosion behave as a pronounced anisotropy with a maximum along the laser polarization vector,[14,15] which may be attributed to the maximal ionization probability when the molecule axis is parallel to the laser E-field (geometric alignment mechanism). It is also possible that the intense laser pulses distort the internal structure of the molecules, and then induce a polarization within them which in turn interacts with the laser field. Consequently, this sets up a torque which aligns the molecules along the electric field of the laser (dynamic alignment mechanism).[16] The study of intense laser alignment of molecules is a field covering intense laser physics and chemical dynamics with potential applications ranging from high harmonic generation and nanoscale processing to stereodynamics and control of chemical reactions.[17]

Numbers of diatomic and linear triatomic

*Project supported by the National Key Basic Research Special Foundation of China (Grant No TG1999075207), and the National Natural Science Foundation of China (Grant Nos 60378012, 10104003, 10328407 and 90101027).
†Corresponding author. Email: qhgong@pku.edu.cn

molecules such as H_2, N_2, CO, NO, CO_2[6,7,18–21] and some bent triatomic molecules H_2O, NO_2, SO_2 have been studied extensively on the basis of time-of-flight spectra or mass-resolved momentum imaging map.[22–25] However, dissociative ionization and Coulomb explosion for polyatomic molecules lack of investigations. Cornaggia[26,27] reported the Coulomb explosion of some small hydrocarbon molecules and identified the explosion channels using covariance mapping techniques. Castillejo *et al*[28] studied the explosion channels of halogenated ethylenes by intense femtosecond laser pulses and suggested that the energy channelling increased with molecular size. Levis *et al*[29] developed a structure-based tunnelling mechanism to predict intense field laser ionization probabilities of C_2H_n species accurately and emphasized the importance of molecular structure in the interaction of molecules with intense laser fields. Talebpour *et al*[30] suggested that the multiphoton ionization of inner-valence electrons resulted in the excited molecular ions that dissociated rapidly into large fragment ions when they studied the fragmentation of ethylene in an intense femtosecond laser field.

In this paper, we study the dissociative ionization of ethane molecules using a time-of-flight mass spectrometer in an intense laser field ranging from 2.4×10^{15}W/cm^2 to 1.2×10^{16}W/cm^2. For the Keldysh parameter γ=0.28–0.88, field ionization (FI) surpasses multiphoton ionization (MPI) and becomes the predominant molecule-radiation coupling.[31,32] Comparing the experimentally measured average kinetic energy with the theoretically predicted energy of different explosion pathways, we can point out the Coulomb explosion channels.

2. Experimental set-up

The schematic diagram of the experimental system is the same as that in our previous reports.[5,6] A Ti:Sapphire chirped pulse amplifier (CPA) laser system (TSA-10, Spectra-Physics Inc., USA), which delivered 810nm, 130fs laser pulse at a repetition of 10Hz, was employed as the light source. The amplified laser beam was focused by a lens with focus-length 150mm and led into the chamber of the time-of-flight mass spectrometer (TOFMS). To measure the angular distribution, a half-wave plate was inserted into the path of the laser beam to rotate the electric field vector an angle interval of 4°. In the measurement, the polarization angle was defined as the angle between the axis of the TOFMS and the polarization vector of the laser beam.

The apparatus used here was a Wiley-McLaren-type time-of-flight mass spectrometer with a drift tube of 35cm long.[33] The vacuum chamber can be pumped down to an ultimate pressure of 10^{-5}Pa. A C_2H_6 gas sample was introduced into the chamber via a pulsed valve (Park Inc., USA) with a 0.2mm orifice. When the gas sample was admitted, the chamber pressure was maintained at several 10^{-4}Pa to avoid the space-charge effect and pressure broadening of the ion peaks. A microchannel plate assembly was used to detect the ions. The signals were recorded using ultrahigh speed data acquisition card (DP 105, Acqiris Digitizers, Switzerland) at a maximum real-time sampling rate of 1GHz with a load of 50Ω. The measured signals were typically averaged over 256 laser pulses. The pulsed valve, the data acquisition card and the femtosecond laser pulses were in timing, scheduled by a DG535 digital delay and pulse generator (Stanford Research Systems, USA).

3. Results and discussion

3.1. Mass spectra

The typical time-of-flight mass spectrum of ethane irradiated by the laser pulses of 810nm, 130fs, 1.2×10^{16}W/cm^2 is shown in Fig.1. The laser polarization is horizontal in Fig. 1(a) and circular in Fig.1(b).

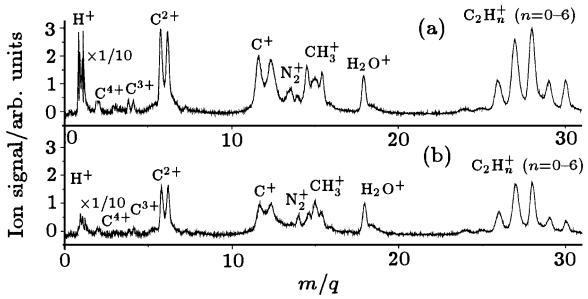


Fig.1. TOF mass spectra of C_2H_6 induced by 810nm, 130fs laser pulses at an intensity of 1.2×10^{16}W/cm^2. (a) Horizontally polarized light. (b) Circularly polarized light.

The strong signals of molecular ions $C_2H_n^+$ (n=0–6) and atomic fragment ions C^{m+} (m=1–4) are observed. The H_2O^+ and H^+ ions are contributed from residual water vapour in the vacuum chamber. The obvious double-peak structure of the atomic fragment ions C^+, C^{2+}, C^{3+} reveals the consequence of Coulomb explosion. The peak with a shorter flight time arises from the ions ejected directly towards the detector, and the peak with a longer flight time, from

the ions ejected in the opposite direction. Great suppression of ionization observed in the case of circular polarization agrees well with the predictions given by field ionization (FI) model. In the FI model, the field ionization probability is the tunnelling efficiency of the electron through the barrier created by the external electric field combined with the molecular potential. The barrier remains static in a duration long enough to allow the electron to penetrate it in the case of linearly polarized light. However, in the case of circularly polarized light with the rotating E-field vector, the electrons have not enough time to traverse the barrier before the laser electric vector changes. Therefore, the ionization is strongly suppressed in the use of the circularly polarized laser light.

3.2. Kinetic energy release (KER) and angular distribution of atomic ions

The double-peak structure of atomic ions in the mass spectrum shown in Fig.1 indicates that they originate from the Coulomb explosion of highly charged molecular ions. The kinetic energy of those ions can be determined by the formula:

$$E_{\text{kineticenergy}} = \frac{(U_1 - U_2)^2}{8md^2} q^2 \Delta t^2,$$

where U_1 is the potential of the repeller plate, U_2 the potential of the first acceleration plate, d the distance between these plates, q the charge of the ions and Δt is the difference in the arrival times between forward and backward ejected ions. The experimentally measured kinetic energy of C^{m+} (m=1–3) for different laser intensities ranging from 2.4×10^{15}W/cm^2 to 1.2×10^{16}W/cm^2 is shown in Fig.2. It can be noticed that the average kinetic energy for the above atomic ions increases with laser intensity, which is consistent with our previous measurements on N_2.[6]

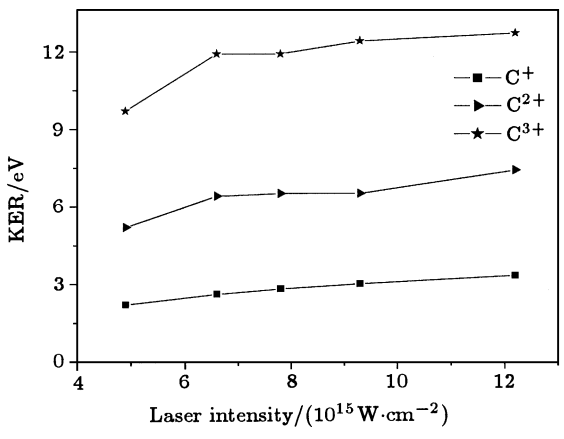


Fig.2. Variation of kinetic energy of C^{m+} determined by the peak splitting method with laser intensity.

Theoretically, we can predict the kinetic energy by solving the classical Newton equations starting with the critical internuclear distance $R_c = 2R_e$. The equilibrium internuclear distance was taken as 0.154nm between C–C and 0.110nm between C–H.[34] The bond angles of H–C–C and H–C–H are 110.1° and 108.8°, respectively. The calculated values without regard to laser intensity are shown in Table 1. The notation (p, q) stands for the Coulomb explosion channel (C^{p+}, C^{q+}).

Table 1. Experimentally measured average kinetic energy for C^+, C^{2+} and C^{3+} at a laser intensity of 1.2×10^{16}W/cm^2 and calculated atomic ion kinetic energy by solving the classical Newton equations at $R_c = 2R_e$.

Ions	E_{exp}/eV	Channels (p, q)	E/eV (theoretical)
C^+	3.3	(1, 1)	2.3
		(1, 2)	4.4
		(1, 3)	6.4
C^{2+}	7.4	(2, 1)	4.9
		(2, 2)	9.2
		(2, 3)	13.4
C^{3+}	12.7	(3, 1)	7.6
		(3, 2)	14.3

Comparing with the experimentally measured kinetic energy at a laser intensity of 1.2×10^{16}W/cm^2, we can deduce that C^{2+} originated from two channels $C_2^{3+}\rightarrow C^+ + C^{2+}$ and $C_2^{4+}\rightarrow C^{2+} + C^{2+}$, and that C^{3+} came from $C_2^{4+}\rightarrow C^+ + C^{3+}$ and $C_2^{5+}\rightarrow C^{2+} + C^{3+}$. While C^+ ion was born of $C_2^{2+}\rightarrow C^+ + C^+$, $C_2^{3+}\rightarrow C^+ + C^{2+}$ and dissociative channel $C_2^+\rightarrow C^+ + C$, which will be described in detail in the following content. Moreover, it is noted that the higher charge state channel is preferable as the laser intensity is increased.

We measured the angular distributions of fragment ions by inserting a half-wave plate into the laser beam path to rotate the electric field vector an angle interval of 4°. The angular distributions of atomic ions C^+, C^{2+}, C^{3+} and a molecular ion $C_2H_4^+$ as a representative are shown in Fig.3.

The molecular ion $C_2H_4^+$ exhibits uniform signal intensity for all the polarized angles (isotropic). In addition to a strong underlying isotropic component, the C^+ ion exhibits anisotropy, whereas C^{2+}, C^{3+} ions are highly anisotropic, with a maximum along the laser polarization axis and a minimum perpendicular to it. The isotropic component of C^+ arises from the fragmentation of the singly charged molecular ions, for example $C_2^+\rightarrow C^+ + C$. The dissociation of singly charged molecular ion is not a Coulomb explosion process and

only imparts a small kinetic energy to the C^+ and the neutral counter-fragment. Conversely, the distributions for C^{2+} and C^{3+} are isotropic. These ions are derived from the fragmentation of highly ionized state molecular ions resulting from Coulomb explosion. This process brings great energy to these atomic fragment ions. The FWHM (full width at half maximum) values of angular distributions for C^+, C^{2+}, and C^{3+} are 111.9°, 90.2°, 88.6° respectively, which is consistent with the results in earlier work on CO molecules.[35]

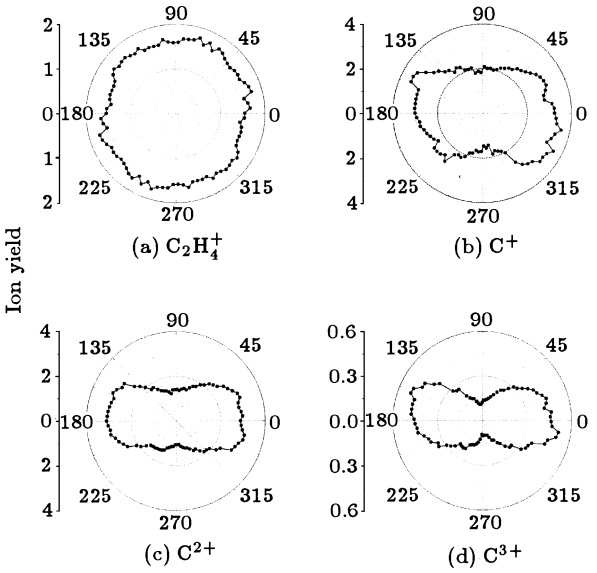


Fig.3. Angular distribution of the ions observed in the MEDI of C_2H_6 at a laser intensity of 1.2×10^{16}W/cm^2.

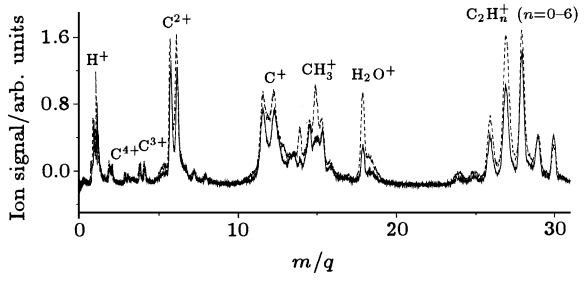


Fig.4. Mass spectra of C_2H_6 in the parallel linearly polarized laser field (solid line) at an intensity of 6.3×10^{15}W/cm^2, and in the circularly polarized laser field (dashed line) at an intensity of 1.2×10^{16}W/cm^2.

Both linearly polarized laser and circularly polarized laser were used to evaluate the contributions of the dynamic and geometric alignment to the observed anisotropic angular distribution of the exploding fragments. Figure 4 depicts the mass spectra obtained using the parallel linearly polarized laser field (solid line) and the circularly polarized laser field (dashed line).

The laser intensity is approximately doubled in the case of circularly polarized laser to ensure that the field amplitude is identical in the two polarized states. The ion yield of C^+ for circular polarization is 1.6 times that for parallel polarization. For C^{2+} and C^{3+}, the factors are 1.3 and 1.1 respectively. The results are greatly disagreed with the prediction of dynamic alignment, which indicates the ion yields should be highly suppressed in the circularly polarized light compared with the linear polarized case under the condition of the same field amplitude. Therefore, we conclude that geometric alignment is responsible for the distinct anisotropic angular distributions. The additional ion yield in the circularly polarized laser case should be contributed by the perpendicular field component, which has equal amplitude but its phase is shifted by $\pi/2$.

4. Conclusions

The interaction of the polyatomic molecule C_2H_6 with an intense femtosecond laser field was experimentally investigated with a time-of-flight mass spectrometer and a chirped pulse amplifier laser. The kinetic energy of atomic ions from Coulomb explosion was measured at different laser intensities ranging from 2.4×10^{15}W/cm^2 to 1.2×10^{16}W/cm^2. Atomic fragment ions C^{2+} and C^{3+} originated from multiple Coulomb explosion channels. In addition, a portion of atomic ions C^+ was born of the dissociation of singly charged molecular ions. The geometric alignment is believed to be responsible for the pronounced anisotropy of the atomic ions angular distribution.

References

[1] Frasinski L J, Colding K and Hatherly P A 1989 *Phys. Lett.* A **142** 499

[2] Cornaggia C 1995 *Phys. Rev.* A **52** R4328

[3] Cornaggia C, Schmidt M and Normand D 1994 *J. Phys. B: At. Mol. Opt. Phys.* **27** L123

[4] Nakashima N *et al* 2000 *J. Photochem. Photobiol. C.* **1** 131

[5] Ren H Z *et al* 2003 *J. Phys. B: At. Mol. Opt. Phys.* **36** 2179

[6] Wu C Y *et al* 2002 *Appl. Phys.* B **75** 91

[7] Cornaggia C *et al* 1991 *Phys. Rev.* A **44** 4499

[8] Normand D, Lompré L A and Cornaggia C 1992 *J. Phys. B: At. Mol. Opt. Phys.* **25** L497

[9] Posthumus J H, Giles A J, Thompson M R and Codling K 1996 *J. Phys. B: At. Mol. Opt. Phys.* **29** 5811
[10] Posthumus J H *et al* 1996 *J. Phys. B: At. Mol. Opt. Phys.* **29** L525
[11] Posthumus J H, Frasinski L J, Giles A J and Codling K 1995 *J. Phys. B: At. Mol. Opt. Phys.* **28** L349
[12] Chelkowski S and Bandrauk A D 1995 *J. Phys. B: At. Mol. Opt. Phys.* **28** L723
[13] Brewczyk M and Frasinski L J 1991 *J. Phys. B: At. Mol. Opt. Phys.* **24** L307
[14] Couris S, Koudoumas E, Leach S and Fotakis C 1999 *J. Phys. B: At. Mol. Opt. Phys.* **32** L439
[15] Graham P *et al* 1999 *J. Phys. B: At. Mol. Opt. Phys.* **32** 5557
[16] Posthumus J H *et al* 1998 *J. Phys. B: At. Mol. Opt. Phys.* **31** L553
[17] Stapelfeldt H and Seideman T 2003 *Rev. Mod. Phys.* **75** 543
[18] Thompson M R *et al* 1997 *J. Phys. B: At. Mol. Opt. Phys.* **30** 5755
[19] Hering Ph and Cornaggia C 1999 *Phys. Rev.* A **59** 2836
[20] Lavancier J *et al* 1991 *Phys. Rev.* A **43** 1461
[21] Chen J X *et al* 2003 *Chin. Phys.* **13** 24
[22] Bhardwaj V R, Safvan C P, Vijayalakshmi K and Mathur D 1997 *J. Phys. B: At. Mol. Opt. Phys.* **30** 3821
[23] Iwamae A, Hishikawa A and Yamanouchi K 2000 *J. Phys. B: At. Mol. Opt. Phys.* **33** 223
[24] Hishikawa A *et al* 1998 *Chem. Phys. Lett.* **282** 283
[25] Hishikawa A *et al* 1998 *Chem. Phys.* **231** 315
[26] Cornaggia C, Normand D and Morellec J 1992 *J. Phys. B: At. Mol. Opt. Phys.* **25** L415
[27] Cornaggia C, Schmidt M and Normand D 1995 *Phys. Rev.* A **51** 1431
[28] Castillejo M *et al* 2002 *Chem. Phys. Lett.* **353** 295
[29] Prall B S, Dewitt M J and Levis R J 1999 *J. Chem. Phys.* **111** 2865
[30] Talebpour A, Bandrauk A D, Yang J and Chin S L 1999 *Chem. Phys. Lett.* **313** 789
[31] Keldysh L V 1965 *Sov. Phys. JETP* **20** 1307
[32] Wu C Y and Gong Q H 2001 *Chin. Phys.* **10** 814
[33] Wiley W C and McLaren I H, 1955 *Rev. Sci. Instr.* **26** 1150
[34] Nicholson A J C 1965 *J. Chem. Phys.* **43** 1171
Al-Joboury M I and Turner D W 1964 *J. Chem. Soc. London* **44** 34
[35] Hatherly P A *et al* 1990 *J. Phys. B: At. Mol. Opt. Phys.* **23** L291